Comparative Medicine
Copyright 2022
by the American Association for Laboratory Animal Science

Vol 72, No 4
August 2022
Pages 267–272

Case Study

Semi-quantitative Assessment of Alzheimer's-like Pathology in Two Aged Polar Bears (*Ursus maritimus*)

Katherine L Lucot,[1,2] Syed A Bukhari,[1] Ebony D Webber,[3,4] T Adam Bonham,[3] Corinna Darian-Smith,[3] Thomas J Montine,[1] and Sherril L Green[3,*]

Age-associated neurodegenerative changes, including amyloid β (Aβ) plaques, neurofibrillary tangles (NFTs), and amyloid angiopathy comparable to those seen in the brains of human patients with Alzheimer's disease (AD), have been reported in the brains of aged bears. However, the significance of these findings in bears is unclear due to the difficulty in assessing cognitive impairment and the lack of standardized approaches for the semiquantitative evaluation of Aβ plaques and NFTs. In this study, we evaluate the neuropathologic changes in archival brain tissue of 2 aged polar bears (*Ursus maritimus*, ages 28 and 37) using the National Institute of Aging-Alzheimer Association (NIA-AA) consensus guidelines for the neuropathologic assessment of Alzheimer's Disease (AD). Both bears had an Aβ (A) score of 3 of 3, Braak stage (B score) of 2 of 3, and neuritic plaque (C) score of 3 of 3. These findings are consistent with the neurodegenerative changes observed in brains of patients with AD. The application of NIA-AA consensus guidelines, as applied to the neuropathologic assessment of the aged bears in this report, demonstrates the use of standardized semiquantitative assessment systems for comparative, translational studies of aging in a vulnerable wildlife species.

Abbreviations: Aβ, amyloid beta; AD, Alzheimer's disease; B score, Braak stage; CERAD, Consortium to Establish a Registry for Alzheimer's Disease; NIA-AA, National Institute of Aging-Alzheimer Association; NFTs, Neurofibrillary tangles

DOI: 10.30802/AALAS-CM-22-000036

Introduction

Neurofibrillary tangles (NFTs) and neuritic and amyloid β (Aβ) plaques are all age-associated neurodegenerative changes described in the brains of humans and in the brains of many animal species, including bears of the *Ursidae* family, genus *Ursus*.[3,16,18] Polar bears (*Ursus maritimus*) are members of this genus and live up to 20 y in the wild and 45 y under managed care.[15] The Aβ plaques and NFTs described in aged polar bears are comparable to neuropathologic changes seen in Alzheimer's disease (AD) patients.[3,16,18] However, reports describing Aβ plaques and NFTs in brain tissue from aged polar bears often do not include complete medical histories or descriptions of behavioral changes that suggest cognitive impairment,[3,16,18] and no postmortem studies have used standardized, semiquantitative postmortem scoring systems to evaluate neuropathologic changes in the aged polar bear brain.

In the late 1980s, the Consortium to Establish a Registry for Alzheimer's Disease (CERAD) developed a standardized, simple, semiquantitative scoring protocol for assessment of the frequency, or burden, of neuritic plaques in the neocortex using silver-based staining methods.[14] The CERAD score, coupled with the patient's age and clinical signs of dementia, was intended to provide a level of certainty for the diagnosis of AD and cognitive decline and to overcome inconsistent criteria and variability between reporting laboratories. In 1991 and 2002, respectively, Braak and colleagues[2] and Thal and colleagues[19] established 2 additional semiquantitative scoring systems intended to further refine the diagnosis and evaluate the neuropathologic changes: the Thal Aβ phase (TAP) scoring system, which focuses on the detection and location of immunopositive amyloid plaques in cortical and subcortical areas of the brain (Table 1 and Figure 1), and the Braak staging system, which focuses on the location and progression of neurofilament pathology, especially of NFTs (Table 2 and Figure 2) using silver-iodate staining techniques. In 2012 Montine and colleagues[10] collated these scoring systems and established criteria to assess AD-associated neuropathologic changes and produced an 'ABC' scoring system (Table 3) that incorporates histopathologic assessment of Aβ plaques (A score) using the Thal Aβ amyloid plaque scoring system, Braak staging (B score) of neurofibrillary tangles (Table 4), and the CERAD (C score) scoring of the neuritic plaque burden (Table 5). These semiquantitative scoring systems have reduced diagnostic inconsistencies and established that higher plaque and NFT scores correlate with a greater likelihood of AD and cognitive impairment.[10] Here we report the use of the Thal Aβ, Braak staging, CERAD, and ABC semiquantitative scoring systems to assess archival brain specimens from 2 aged polar bears.

Received: 07 Apr 2022. Revision requested: 14 May 2022. Accepted: 27 May 2022.
[1]Department of Pathology, Stanford University School of Medicine, Stanford, California, [2]UC Davis Health, Sacramento, California, [3]Department of Comparative Medicine, Stanford University School of Medicine, Stanford, California, [4]Champions Oncology, Rockville, Maryland
[*]Corresponding author. Email: sherril@stanford.edu

Table 1. Thal Aβ Phasing (TAP)[19]

Thal Phase	Location of Aβ deposits
1	Aβ deposits are in the frontal, parietal, temporal, or occipital neocortex. All other regions of the brain do not have Aβ deposits. Deposits can appear focally in small groups, or as diffuse plaques in layers II, III, IV, and V.
2	Aβ deposits now appear in the entorhinal region, CA1, and the insular cortex. In addition, Aβ deposits can occur in the amygdala, the cingulate gyrus, the presubicular region, and the molecular layer of the fascia dentata. Aβ is also seen in the regions defined in phase 1.
3	Aβ can be found in the following subcortical regions: caudate nucleus, putamen, claustrum, basal forebrain nuclei, substantia innominata, thalamus, hypothalamus (including the mamillary body), lateral habenular nuclei, and white matter. Aβ is also seen in the regions defined in phases 1 and 2.
4	Additional Aβ deposits in the inferior olivary nucleus, the reticular formation of the medullla oblongata, and the substantia nigra, CA4, the central gray of the midbrain, the colliculi superiores, and inferiores, and the red nucleus. β is also seen in the regions defined in phases 1 through 3.
5	In addition to the Aβ deposits seen in the previous 4 phases, Aβ can now be found in the reticular formation of the pons, the pontine nuclei, the central and dorsal raphe nuclei, the locus coeruleus, the parabrachial nuclei, the dorsal tegemental nucleus, the reticulotegmental nucleus of the pons, and the cerebellum.

Case Reports

These studies were conducted on archival polar bear brain tissues under approval of the institutional animal use and care committee. Formalin fixed brain tissues from 2 aged polar bears were retrieved from the necropsy archives at Stanford University, Department of Comparative Medicine. Both bears had been housed for several decades at AZA-accredited zoos and were under managed care. No additional clinical information, other than that described below was available. The clinical information below was described in the necropsy request forms that were filed with the archival tissues.

The first bear (PB1), a 37-y-old female, displayed progressive disorientation, failure to recognize food, and hind limb weakness. The bear was euthanized on Jan 27, 1997 after 2 wk of supportive care including antibiotics, vitamin supplements, and corticosteroids. The second bear (PB2), a 28-y-old male, was euthanized on Oct 5, 1984 due to chronic weight loss, depression, and suspected chronic pulmonary disease. Postmortem intervals between euthanasia and necropsy were approximately 1 h for both bears.

Materials and Methods

The bears were euthanized at their respective zoos and the brains were collected on location. Whole brains from each bear were immersed in 10% neutral-buffered formalin. Coronal sections through an entire cerebral hemisphere were blocked, dehydrated in a series of alcohols and xylenes (xylene: 100%, 95%, and 70% for 5 min each), paraffin embedded, and cut

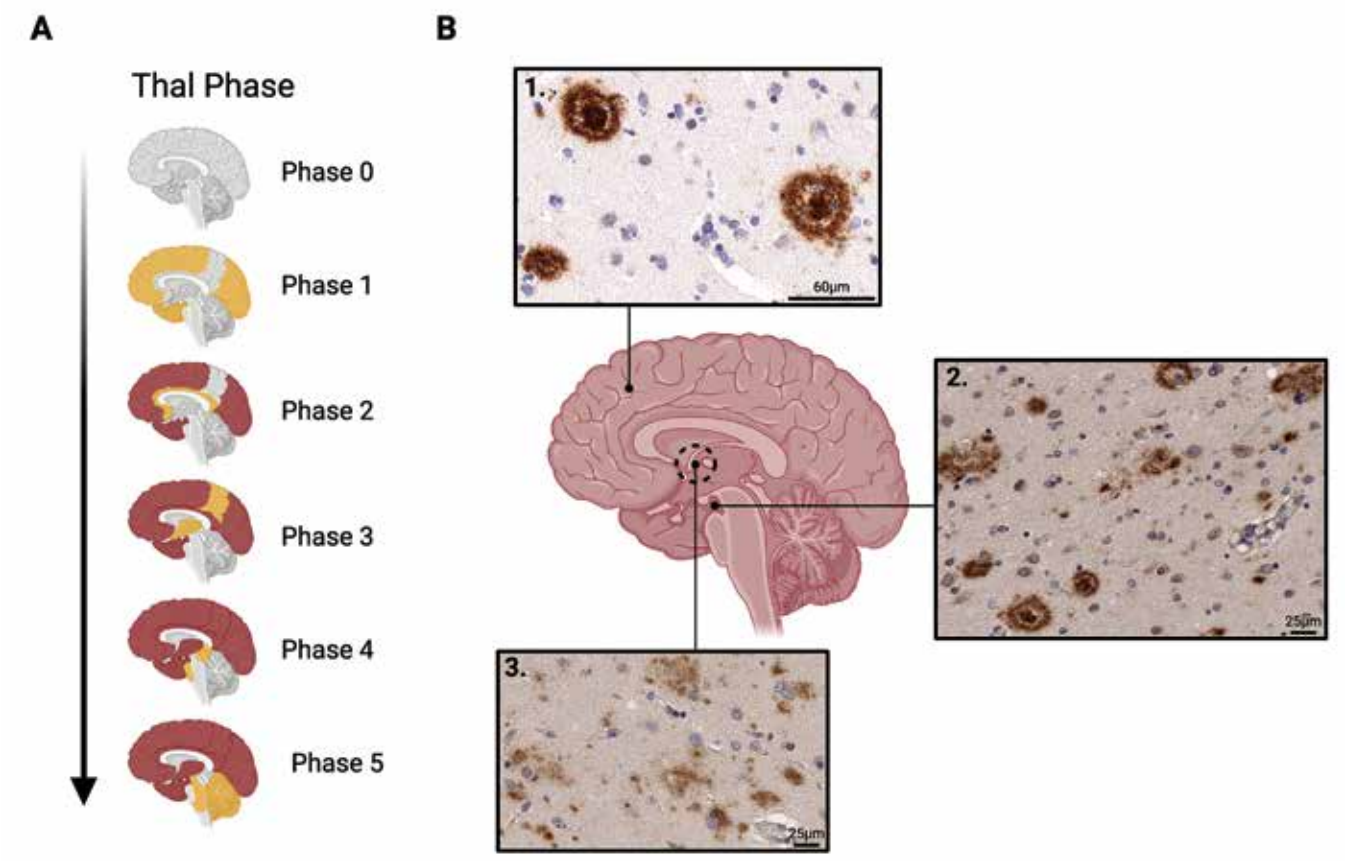

Figure 1. A) Thal Aβ phase and progression of amyloid-β deposition in a human Alzheimer's disease brain. Yellow signifies novel pathologic change; red signifies regional progression of amyloid-β accumulation. B) Immunoreactive amyloid-β plaques in an Alzheimer's disease brain. B1) Plaques present in the middle frontal gyrus. B2) Plaques present in the hippocampus. B3) Diffuse plaques present in the basal ganglia; dashed circle indicating subcortical nuclei embedded deep within the brain.

Table 2. Braak Staging[2] of Neurofibrillary Tangles (NFTs), Neuritic Plaques (NP), and Neuropil Threads (NTs)

Braak Stage	Location of Neurofibrillary Tangles
I *Transentorhinal Stage*	NFTs are confined to the transentorhinal region of the cortex. The transentorhinal projection neurons are the first nerve cells to develop NFTs and NT.
II *Transentorhinal Stage*	Stage I, in addition to numerous NFTs and NTs in the transentorhinal cortex. The CA1 of the hippocampus is affected by some NFTs. The magnocelluar forebrain nuclei and the antero-dorsal nucleus of the thalamus only show mild changes.
III *Limbic Stage*	Involvement of the transentorhinal and entorhinal regions, CA1, pyramidal cells of the subiculum, possible mild changes in the isocortex, and within layers III and V in basal portions of frontal, temporal, and occipital association areas.
IV *Limbic Stage*	The transentorhinal and entorhinal cortices are severely affected. CA1 contains numerous NFTs. Mild involvement of the subiculum and modest affection of CA4-nerve cells. The isocortex is mildly affected. The amygdala has many NP, while NFTs and NTs predominate the basolateral nuclei. Low isocortical involvement.
V *Isocortical Stage*	Severe changes to the transentorhinal and entorhinal cortices. Virtually all regions of the hippocampus are involved. The isocortex is severely affected. The antero-dorsal nucleus of the thalamus reveals considerable loss of nerve cells. The antero-ventral nucleus displays initial neurofibrillary changes. Slight changes in the lateral tuberal nucleus of the hypothalamus and in the pars compacta of the substantia nigra can be seen.
VI *Isocortical Stage*	All changes are even more pronounced. The hippocampus is highly affected. Large numbers of NFT-bearing granule cells in the fascia dentata differentiate stage V from stage VI. All isocortical areas are very severely affected. The extrapyramidal system is now involved. The striatum contains NFTs.

into 6-µm sections in preparation for the histologic studies as described below.

For the purpose of methodological controls, human brain samples were obtained through the Stanford Alzheimer's Disease Research Center (ADRC; NIH/NIA P50ZG047366). Collection of the brain tissue for the ADRC was approved by the Stanford Institutional Review Board and written consent had been obtained from all subjects. The ADRC approved the use of the brain tissues for this study. The analysis was carried out on deidentified patient samples. All subjects were free of acute infectious disease. Human brain samples were obtained from archival tissues from a 96-y-old female, 99-y-old female, and 100-y-old male, all diagnosed with AD, and from a 101-y-old female diagnosed with dementia, but not AD. The formalin-fixed human brain samples were processed as described above. Bear and human brain tissue samples were processed, sectioned, and slides were stained in parallel in the Human Pathology/Histology Service Center laboratory at Stanford University, as previously described,[4,10,13] minimally including sections of the neocortex, neostriatum, and cerebellum.[10]

Bielschowsky silver staining. Tissues were processed for Bielschowsky silver staining, a single stain that detects NFTs, amyloid and neuritic plaque components based on methods previously described.[4,13] Bear and human brain sections were baked at 65 °C overnight before rehydration in distilled water (3 changes). Slides were submerged in preheated 20% silver nitrate solution (silver nitrate and distilled water) and baked at 37 °C for 15 min, then subsequently washed in distilled water (3 changes). Slides were then placed in ammoniacal silver solution (20% silver nitrate, and ammonium hydroxide) for 10 min at 37 °C before being developed for 1 to 5 min in a working developer solution (formaldehyde 37% to 40%, citric acid, nitric acid, distilled water, ammonium hydroxide, and distilled water). After development, slides were placed in a 'stop bath' of 5% sodium thiosulfate for 2 min, washed in distilled water (3 changes), and then dehydrated.

Immunohistochemistry. Tissues were processed for anti-β-amyloid immunohistochemistry as adapted from previously described methods.[1,3,6,8,9] Both bear and human brain sections were incubated at 65 °C overnight before rehydration in a series of xylenes and alcohols (xylenes, xylenes, 100%, 95%, and 70% for 5 min each). Sections were pretreated with 0.6% H_2O_2, washed with tris-buffered saline wash buffer (1× - TBS Wash Buffer; Cat. #00-4954-56, Thermo Fisher Scientific, Waltham, MA, 02451), incubated with 2.5% normal horse serum (ImmPRESS HRP Horse Anti-Mouse IgG Polymer Detection Kit, peroxidase (MP-7402; Vector Laboratories, Burlingame, CA, 94010, USA), and then incubated overnight at 4 °C with the primary antibody diluted in TBS (anti-β-amyloid, 17-24 Antibody (1:2,000; Cat. #800701, BioLegend, San Diego, CA, 92121) as previously described.[2] Sections were washed and incubated at room temperature for one hour with the secondary antibody (horse anti-mouse) from the ImmPRESS HRP kit (Vector Laboratories). Reaction product was developed with 0.05% 3,3'-Diaminobenzidine (DAB) tetrahydrochloride (Cat. #D5905, Sigma-Aldrich; Burlington, MA, 01803) 0.03% H_2O_2 for one minute at room temperature. Washes were performed in TBS, with the final wash completed in 0.1 M Tris HCl (pH 7.4). Sections were dehydrated (70%, 95%, 100% xylene, for 5 min each), and coverslipped with Entellan (Cat. #107960, Sigma-Aldrich). Coverslipped sections were examined with a digital slide scanning program (Hamamatsu NanoZoomer 2.0RS, Hamamatsu Corporation, Bridgewater, NJ, 08807).

Semiquantitative scoring of the brains. Bear brain tissue sections were grossly evaluated by a veterinarian (SG) and a comparative anatomist (CDS), and human and bear brains scored independently by a board-certified pathologist (TM) and by a research scientist (SB) with experience in the TAP, Braak, CERAD, and ABC assessment systems. Specifically, all brain tissue sections were evaluated and scored for accumulation of Aβ plaques using TAP and a 4-point 'A' scoring system (Table 3),[2,19] and assessed for tau aggregates, as seen in the form of NFTs, using a 4-point 'B' scoring system (Table 4) modified from Braak and Braak.[2] The CERAD score for neuritic plaques was determined by TM and SB and based on assessment of the frequency of neuritic plaques in neocortex (Table 5).[10] Staging of amyloid accumulation, neurofibrillary aggregates, and neuritic plaques were reported in the form of an ABC score that was translated into one of 4 levels of AD neuropathologic change (ADNC): Not AD, Low, Intermediate, or High AD severity.

Results

The results of silver stains, immunohistochemistry, and the semiquantitative scoring of human and bear brain tissues are summarized in Table 6. The 2 coauthors (TM and SB) who scored the brains had 100% agreement. Bielschowsky silver stains of bear sections (Figure 3) revealed neuritic plaques throughout both brains with a C score of 3 of 3. Two AD patients had C

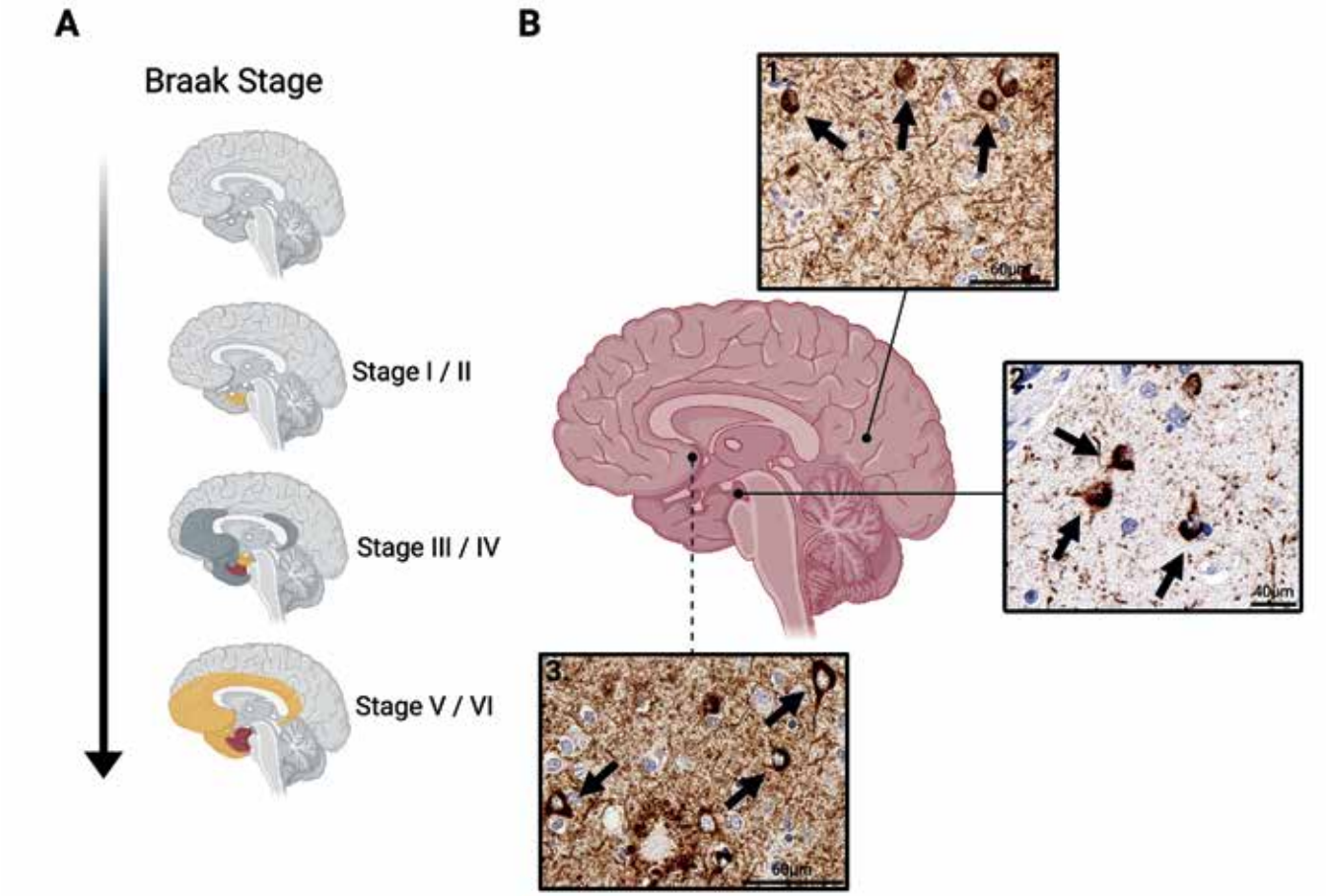

Figure 2. A) Braak staging in a human Alzheimer's disease brain. Yellow signifies novel pathologic change; red signifies regional progression of neurofibrillary degeneration. B) Immunoreactive phosphor-tau neurofibrillary tangles in an Alzheimer's disease brain. B1) Neurofibrillary tangles present in the inferior parietal lobe (marked by black arrows). B2) Neurofibrillary tangles present in the hippocampus (marked by black arrows). B3) Neurofibrillary tangles present in the superior and middle gyrus (marked by black arrows), with the dashed line signifying the pathology is lateral to the location shown.

Table 3. ABC Scoring System for Severity of AD Neuropathologic Change[13]

	B: NFT score (Braak stage)			
A: A β amyloid plaque score (Thal phases)	**B0 or B1 (None or I/II)**	**B2 (III/IV)**	**B3 (V/VI)**	**C: Neuritic plaque score (CERAD)**
A0 (0)	Not*	Not	Not	C0 (none)
A1 (1/2)	Low	Low	Low	C0 or C1 (none to sparse)
	Low	Intermediate	Intermediate	C2 or C3 (mod. To freq.)
A2 (3)	Low	Intermediate	Intermediate	Any C
A3 (4/5)	Low	Intermediate	Intermediate	C0 or C1 (none to sparse)
	Low	Intermediate	High	C2 or C3 (mod. To freq.)

*Not = Not Alzheimer's Disease

Table 4. ABC Score for Braak and Braak NFT Staging[13]

Score	Staging
B0	No NFTs
B1	Braak Stage I or II
B2	Braak Stage III or IV
B3	Braak Stage V or VI

Table 5. ABC Score for CERAD Neuritic Plaque Score[13]

Score	CERAD Score
C0	No Neuritic Plaques
C1	CERAD Score Sparse
C2	CERAD Score Moderate
C3	CERAD Score Frequent

scores of 3, one AD patient had a C score of 2, and one aged human patient without dementia had a C score of 0. Silver-impregnated NFTs were observed in the hippocampal formation (CA subfields and entorhinal cortex) in the same location in the AD patient brains and in the brains of both bears (Figure 3). A B score was 2 of 3 in 2 human brains and 3 of 3 in the other 2 human brains. Polar bear 1 had a B score of 3 of 3 and PB2 had a B score of 2 of 3. Amyloid plaques were notably absent in the human cerebellum; however, they had progressed to the cerebellum of both bears resulting in an A score of 3 of 3.

Table 6. Aged Polar Bears, AD Patients and Non-AD Dementia Patient Control TAP, Braak, and CERAD scores

Subject	Species	Age	Sex	TAP	Braak	CERAD	A	B	C	Diagnosis
PB1	Polar Bear	37	F	4	5	3	3	3	3	BC
PB2	Polar Bear	28	M	5	4	3	3	2	3	BC
H1	Human	96	F	5	6	3	3	3	3	AD
H2	Human	99	F	4	4	2	3	2	2	AD
H3	Human	100	M	4	5	3	3	3	3	AD
H4	Human	101	F	0	4	0	0	2	0	NADD

Abbreviations: PB, Polar Bear; BC, Behavioral Change; H, Human; AD, Alzheimer's Disease; NADD, Non-Alzheimer's Disease Dementia.

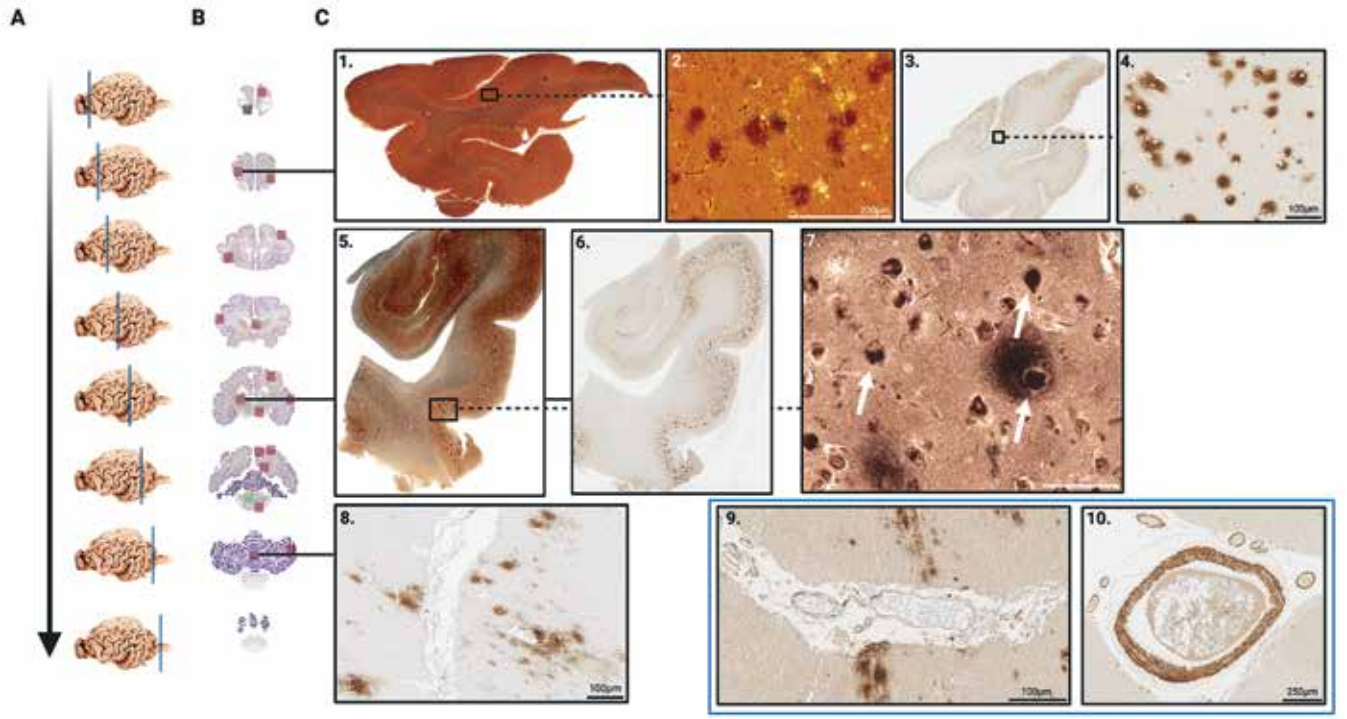

Figure 3. Polar bear brain atlas showing progression of amyloid-β and tau pathologic change throughout the brain. A) Blue bar shows location of coronal cross sections as progressing from the rostral to caudal pole. B) Red boxes delineate pathologic change, gray boxes indicate region was not sampled, green box indicates no pathologic change. C1–2) Silver-stained prefrontal cortex with zoomed in image of diffuse plaques. C3–4) Amyloid-β immunoreactivity of the prefrontal cortex indicating extensive plaque deposition. C3 Also shows amyloid-β immunoreactivity within the cortical ribbon of the cerebral cortex. C5–6) Silver-stained and amyloid-β immunoreactivity of the hippocampus and amygdala, showing extensive plaque deposition. C7) Silver-stained hippocampus showing neurofibrillary tau tangles (marked by white arrow). C8) Amyloid-β immunoreactivity of the cerebellum, showing diffuse plaques, confirming Thal phase 5/5. C9–10) Amyloid-β immunoreactivity of cerebral blood vessels showing extensive cerebral amyloid angiopathy in different regions of the brain (C9 – cerebellum; C10 – hippocampus). Brain atlas images were reproduced (or adapted) with permission from http://brainmuseum.org. Specimens used for this publication are from the Department of Health Affairs Neuroanatomical Collections Division of the National Museum of Health and Medicine, the University of Wisconsin and Michigan State Comparative Mammalian Brain Collections supported by the US National Science Foundation.

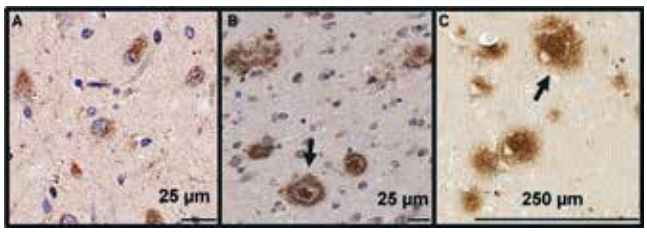

Figure 4. A) Anti-Aβ staining in the hippocampus of the non-AD dementia patient, showing a lack of immunoreactive Aβ plaques. B) Immunoreactive Aβ plaques in the hippocampus of an Alzheimer's disease brain. C) Immunoreactive Aβ plaques in the hippocampus of an aged polar bear. Arrows identify an example of an Aβ plaque.

Immunohistochemistry (Figure 3) identified numerous Aβ plaques in the bear neocortex, allocortex, striatum, and cerebellum, and both bears had an A score of 3. Both bears had evidence of extensive cerebrovascular amyloid angiopathy (Figure 3). All AD brain samples had A scores of 3, while the human control brain had an A score of 0 (Figure 4). Similarly, the frequency of Aβ plaques in the caudate and putamen of AD brains and in both polar bear brains was less than in the neocortex. The AD and the polar bear brains all had B scores of 2 or higher. In this study population, non-Alzheimer's disease dementia was diagnosed in one human patient and AD in the other 3. Behavioral changes were observed in both polar bears, although both bears had underlying comorbidities that may have contributed to these changes.

Discussion

Here we report the use of the current consensus NIA-AA guidelines for the neuropathologic assessment of AD to evaluate archival brain tissues from 2 aged polar bears (*Ursus maritius*). Components of these guidelines have been used to assess

age-related and AD-like pathologic changes in nonhuman primate models of AD[11] and in aging felines,[7] but to date have not been applied to polar bears. The neuropathological findings reported here are in agreement with previous descriptive studies reporting Aβ plaques and neuritic plaques in aged polar bears. The use of a semiquantitative scoring system further refines reporting of the pathologic findings and allows for a more exact analysis.

The scoring systems used here can be correlated with cognitive decline in human patients, even when medical histories are incomplete and are a useful diagnostic aid.[3,10] Unfortunately, the medical histories of the polar bears in this report are also incomplete. Furthermore, it is difficult in veterinary medicine to obtain brain imaging studies using MRI, or CT, or to collect and analyze CSF biomarkers or to conduct neurologic examinations (beyond what can be observed from a distance) from polar bears antemortem. Our case study is further limited by the lack of availability of archived brain tissue from age-matched, zoo-housed polar bears whose brains showed no neurodegenerative pathology. Thus, any correlation between the AD-like pathology and the bears' observed behavioral changes, particularly disorientation, depression, and failure to recognize food (as reported by the zoo staff), would be speculative. However, these observed behavioral changes, along with the bears' high A, B, and C scores suggests that some degree of cognitive impairment may have been present and is related, at least in part, to the neuropathology. Reports of other specific neurologic diseases that might also cause cognitive impairment in polar bears are rare, but differential diagnoses should also include equine herpes virus 9,[5,8] suid herpes virus,[1] West Nile virus,[6] and rabies.[12,17]

Polar bears are currently listed as a vulnerable species by the IUCN,[20] are under significant stress due to climate change, and face ongoing population decline.[15] Bears experience many age-related changes, physically and behaviorally, and under managed care in zoos, are living longer than ever.[9] This observation applies especially to polar bears, given their biologic propensity for longevity. Refinement, standardization, and application of scoring systems such as those described here are a key to the diagnosis and understanding aging and the associated neuropathologic changes in the brains of this at-risk species.

Conflict of Interest

The author(s) declare(s) they have no conflicts of interest.

Ethics Statement

The authors confirm that the ethical policies of the journal, as noted on the journal's author guidelines page, have been adhered to.

References

1. **Banks M, Torraca LS, Greenwood AG, Taylor DC.** 1999. Aujeszky's disease in captive bears. Vet Rec **145:**362–365. https://doi.org/10.1136/vr.145.13.362.
2. **Braak H, Braak E.** 1991. Neuropathological stageing of Alzheimer-related changes. Acta Neuropathol **82:**239–259. https://doi.org/10.1007/BF00308809.
3. **Cork LC, Powers RE, Selkoe DJ, Davies P, Geyer JJ, Price DL.** 1988. Neurofibrillary tangles and senile plaques in aged bears. J Neuropathol Exp Neurol **47:**629–641. https://doi.org/10.1097/00005072-198811000-00006.
4. **Crookham JN, Dapson RW.** 1991. Hazardous chemicals in the histopathology laboratory: Regulations risks handling & disposal. Battle Creek (MI): Anatech.
5. **Donovan TA, Schrenzel MD, Tucker T, Pessier AP, Bicknese B, Busch MD, Wise AG, Maes R, Kiupel M, McKnight C, Nordhausen RW.** 2009. Meningoencephalitis in a polar bear caused by equine herpesvirus 9 (EHV-9). Vet Pathol **46:**1138–1143. https://doi.org/10.1354/vp.09-VP-0007-D-CR.
6. **Dutton CJ, Quinnell M, Lindsay R, DeLay J, Barker IK.** 2009. Paraparesis in a polar bear (*Ursus maritimus*) associated with West Nile virus infection. J Zoo Wildl Med **40:**568–571. https://doi.org/10.1638/2008-0121.1.
7. **Fiock KL, Smith JD, Crary JF, Hefti MM.** 2020. β-amyloid and tau pathology in the aging feline brain. J Comp Neurol **528:**112–117. https://doi.org/10.1002/cne.24741.
8. **Greenwood AD, Tsangaras K, Ho SY, Szentiks CA, Nikolin VM, Ma G, Damiani A, East ML, Lawrenz A, Hofer H, Osterrieder N.** 2012. A potentially fatal mix of herpes in zoos. Curr Biol **22:**1727–1731. https://doi.org/10.1016/j.cub.2012.07.035.
9. **Krebs BL, Marrin D, Phelps A, Krol L, Watters JV.** 2018. Managing Aged Animals in Zoos to Promote Positive Welfare: A Review and Future Directions. Animals (Basel) **8:**116. https://doi.org/10.3390/ani8070116.
10. **Hyman BT, Phelps CH, Beach TG, Bigio EH, Cairns NJ, Carrillo MC, Dickson DW, Duyckaerts C, Frosch MP, Masliah E, Mirra SS, Nelson PT, Schneider JA, Thal DR, Thies B, Trojanowski JQ, Vinters HV, Montine TJ.** 2012. National Institute on Aging-Alzheimer's Association guidelines for the neuropathologic assessment of Alzheimer's disease. Alzheimers Dement **8:**1–13. https://doi.org/10.1016/j.jalz.2011.10.007.
11. **Latimer CS, Shively CA, Keene CD, Jorgensen MJ, Andrews RN, Register TC, Montine TJ, Wilson AM, Neth BJ, Mintz A, Maldjian JA, Whitlow CT, Kaplan JR, Craft S.** 2019. A nonhuman primate model of early Alzheimer's disease pathologic change: Implications for disease pathogenesis. Alzheimers Dement **15:**93–105. https://doi.org/10.1016/j.jalz.2018.06.3057.
12. **Loewen K, Prins B, Philibert H.** 1990. Northwest Territories. Rabies in a polar bear. Can Vet J **31:**457.
13. **Mirra SS, Hart MN, Terry RD.** 1993. Making the diagnosis of Alzheimer's disease. A primer for practicing pathologists. Arch Pathol Lab Med **117:**132–144.
14. **Morris JC, Heyman A, Mohs RC, Hughes JP, van Belle G, Fillenbaum G, Mellits ED, Clark C.** 1989. The Consortium to Establish a Registry for Alzheimer's Disease (CERAD). Part I. Clinical and neuropsychological assessment of Alzheimer's disease. Neurology **39:**1159–1165. https://doi.org/10.1212/WNL.39.9.1159.
15. **Rode KD, Obbard M, Belikov SE, Derocher AE, Durner GM, Thiemann GW, Tryland M, Letcher RJ, Meyerson R, Sonne C, Jenssen BM, Dietz R, Vongraven D.** 2020. Polar Bear (Ursus maritimus), p 196–212. In: Melletti M, Penteriani V, editors. Bears of the World: Ecology, Conservation and Management. Cambridge: Cambridge University Press.
16. **Selkoe DJ, Bell DS, Podlisny MB, Price DL, Cork LC.** 1987. Conservation of brain amyloid proteins in aged mammals and humans with Alzheimer's disease. Science **235:**873–877. https://doi.org/10.1126/science.3544219.
17. **Taylor M, Elkin B, Maier N, Bradley M.** 1991. Observation of a polar bear with rabies. J Wildl Dis **27:**337–339. https://doi.org/10.7589/0090-3558-27.2.337.
18. **Tekirian TL, Cole GM, Russell MJ, Yang F, Wekstein DR, Patel E, Snowdon DA, Markesbery WR, Geddes JW.** 1996. Carboxy terminal of beta-amyloid deposits in aged human, canine, and polar bear brains. Neurobiol Aging **17:**249–257. https://doi.org/10.1016/0197-4580(95)02062-4.
19. **Thal DR, Rüb U, Orantes M, Braak H.** 2002. Phases of A beta-deposition in the human brain and its relevance for the development of AD. Neurology **58:**1791–1800. https://doi.org/10.1212/WNL.58.12.1791.
20. **Wiig Ø, Amstrup S, Atwood T, Laidre K, Lunn N, Obbard M, Regehr E, Thiemann G.** [Internet]. 2015. Ursus maritimus. The IUCN Red List of Threatened Species. Available at: https://doi.org/10.2305/IUCN.UK.2015-4.RLTS.T22823A14871490.en.